International Journal of Engineering

Journal Homepage: www.ije.ir

Adsorption of Malachite Green from Aqueous Solution by Nanozeolite Clinoptilolite: Equilibrium, Kinetic and Thermodynamic Studies

R. Heydari[a], M. Khavarpour*[b]

[a]Department of Chemical Engineering, South Tehran Branch, Islamic Azad University, Tehran, Iran
[b]Department of Chemical Engineering, Ayatollah Amoli Branch, Islamic Azad University, Amol, Iran

PAPER INFO

Paper history:
Received 29September2017
Received in revised form 23October2017
Accepted 30November2017

Keywords:
Adsorption Kinetics
Thermodynamics
Malachite Green
Nanozeolite Clinoptilolite
Isotherm Models

ABSTRACT

The object of present study was to examine the adsorption potential of nanozeolite clinoptilolite (CP) for the removal of malachite green (MG) from aqueous phase in a batch equilibrium system. SEM, EDX, XRF, XRD and FT-IR techniques of characterization of zeolite were applied. The effects of initial pH solution, adsorbent dose, temperature, contact time and initial MG concentration on adsorption were evaluated. Adsorption experiments were conducted at initial concentrations in the range of 10–50 mg/L and temperatures at 25, 30 and 35°C. MG adsorption uptake was found to increase with an increase in contact time, initial MG concentration and solution temperature. The adsorption equilibrium data revealed the best fit with Koble-Corrigan model. The kinetics of MG on adsorbent followed the pseudo-second-order model. In addition, the assessment of kinetic data depicted that the adsorption rate was controlled by intraparticle diffusion mechanism. The negative values of standard Gibbs free energy represented the spontaneous adsorption at the stated temperature. The positive values of enthalpy and entropy changes also confirmed the increased randomness and endothermic nature of MG adsorption on nanozeolite CP adsorbent. Furthermore, the obtained activation energy showed the physical adsorption process.

***doi**: 10.5829/ije.2018.31.01a.01*

1. INTRODUCTION

Environmental contaminations owing to disposal of industrial effluents pose a major concern. These effluents generated by industries such as food and pharmaceutical industries, textile, pulp and paper, printing and cosmetics contain extensive amount of colored wastewater including acid or base, dissolved solids, toxic compounds, and dyes which is a serious threat for the environment, water quality and human life [1]. Other problems comprise reduction of sunlight penetration into water, increase the unpleasant aesthetic to the ecosystem, interference with gas solubility in water and the aquatic life and enhancement a tendency to chelate metal ions [2]. Dyes also can result in to allergic dermatitis, cancer, skin irritation, mutation, etc. [3]. In general, dyes are poorly biodegradable because of their complicated chemical structure and stability; therefore, it is essential to remove them before depositing into the water bodies [4].

Dyes can be classified into three groups: (i) anionic (reactive, direct and acid dyes), (ii) cationic (basic dyes) and (iii) non-ionic (dispersive dyes) [5]. Basic dyes are the most widely used in many industries which obtained the highest rates of toxicity as well as diazo direct dyes [6]. Malachite green (MG), a cationic triphenylmethane dye, is conventionally used as dye for materials such as wool, silk, cotton, leather, etc. [7]. It has also applications in medical sciences, ceramic industry and in manufacturing of printing inks and paints. It is well known as an antifungal, anti-bacterial, and antiprotozoan agent in animal husbandry and aquacultures [8]. Degradation of MG resulted in to the intermediate products which may have mutagenic and carcinogenic characteristics. Thus, removal of MG from wastewater is of the great interest because of its dangerous effects on environment and human life.

*Corresponding Author's Email:*mkhavarpoor@yahoo.com* (M. Khavarpour)

Please cite this article as: R. Heydari, M. Khavarpour, Adsorption of Malachite Green from Aqueous Solution by Nanozeolite Clinoptilolite: Equilibrium, Kinetic and Thermodynamic Studies, International Journal of Engineering (IJE), IJE TRANSACTIONS A: Basics Vol. 31, No. 1, (January 2018) 1-11

Various attempts have been performed for the removal of dyes from wastewater [9, 10]. Some of these methods which is commonly used are costly, complicated, generated toxic by-products and also not effective because of their stability to light and oxidizing agents [11]. Among treatment technologies, adsorption process have proved to be an effective and attractive process with low cost, sludge-free operation, recovery of the sorbate, ease of operation and selectivity and simplicity of design [12]. Adsorption processes are mainly based on the adsorbent including: (i) activated carbon-based materials (ii) biosorbents, and (iii) inorganic materials. However, activated carbon is used extensively for the removal of dyes [13]. Although, it has extended surface area, large capacity to adsorb dyes, micro-pore structures and high degree of surface reactivity; but it is expensive and has significant regeneration cost while being exhausted [14]. Thus, researches are interested to investigate on efficient, low-cost and easily available kinds of adsorbents.

Recently, biosorbent have been widely studied for dye removal from wastewater. They are less expensive, usually available in large amounts; but they have mainly low efficiency [3]. On the contrary, inorganic materials have mainly mechanical stability and large surface areas [15].

Zeolite is an abundant resource of aluminosilicates which comprises oxygen, hydrogen, silicon and aluminium. It arranged in an interconnecting, open, three-dimensional structure. Zeolite has received remarkable attention and extensive industrial usage because of its wonderful properties such as high cation exchange capability, local and abundant availability, intercrystalline pores and strong acidic sites [16]. The most important naturally occurring zeolite is clinoptilolite. Some reports are available about employing clinoptilolite as an absorbent, a molecular sieve and a food and feed additive because of its large cavity size, and high resistance to extreme temperatures [17]. In addition, use of zeolite in nano size can enhance the properties of adsorbent because of its unusual characteristic and large surface area.

These remarkable properties make zeolite an excellent candidate to use as an adsorbent. However, there is no data about applying nano-sized zeolite for MG removal from aqueous solution. Therefore, the main objective of present research is to use a simple procedure to gain nano-sized zeolite and consequently introduce it as a cheap, natural, easily available and effective adsorbent for the removal of MG as a model compound for basic dyes. Furthermore, we examined for the first time, the adsorption capacity of zeolite obtained from Semnan, Iran, for MG. Batch adsorption studies were carry out to evaluate the effect of various parameters such as pH, initial MG concentration, contact time, sorbent dosage and temperature on removal efficiency. Moreover, kinetic and equilibrium sorption behaviors of the adsorbent were examined. Experimental data were fitted to various isotherm models to achieve the best isotherm to correlate the achieved data. The thermodynamic parameters were also determined.

2. MATERIAS AND METHODS

2.1. Adsorbate The cationic dye, MG oxalate (Color Index: Basic Green 4, Classification Number: 42,000, chemical formula= $C_{52}H_{54}N_4O_{12}$, molecular weight= 927.00, λmax = 618 nm), was purchased from Merck (Darmstadt, Germany). A stock solution of MG was prepared freshly each time by dissolving 250 mg/L MG in deionized water. The experimental solutions were prepared by diluting the MG stock solution with deionized water in accurate proportions to achieve required concentrations. All chemicals and reagents were of analytical grade and used without any further purification. They were obtained from Merck and Sigma-Aldrich (St. Louis, MO, USA).

2.2. Adsorbent The raw zeolite material was obtained from deposits in the region of Semnan. With the aim of obtaining nanozeolite, ball milling of the CP zeolite sample was conducted using a planetary ball mill (PM100; Retsch Corporation). Briefly, experiments was carried out in dry conditions with a time period of about 60 min and 10 balls per 30 g of zeolite powder in a 250 mL stainless steel jar with a protective jacket of zirconium oxide [18].

2. 2. 1. Adsorbent Characterization The chemical composition of raw zeolite was defined by X-ray fraction (XRF). Scanning electron microscope (SEM) pictures were taken using a VEGA II model microscope, (TESCAN Co, Germany) for study of the size and morphology of adsorbent. The presence of functional groups in nanozeoilite was identified by Fourier transform infrared spectroscopy (FT-IR) (using a Perkin Elmer 65 in KBr Matrix, U.S.A). The X-ray powder diffraction (XRD) patterns for nanozeolite were carried out on a Bruker D8 Advance X-ray diffractometer with Cu Kα radiation.

2.3. Batch Adsorption Studies MG adsorption onto nanozeolite in liquid–solid system was preformed. For equilibrium studies, the standard batch technique was used because of its simplicity. The effects of various parameters such as pH, adsorbent dosage, contact time, temperature and initial MG concentration on the adsorption of MG onto nanozeolite were evaluated during different sets of batch experiments. Adsorption experiments were performed in 100mL

beakers by agitating a pre-weighted amount of adsorbent in 50mL of aqueous dye solution of desired concentration. The samples were equilibrated with adsorbent at rotation speed of 150 rpm in incubator shaker (model KS 4000i control, IKA) for the required time period. After adsorption, the samples were withdrawn from the solution at predetermined time intervals. Then, the dye solution was separated from the adsorbent using centrifugation at 5000 rpm for 10 min. The residual concentration of MG in supernatant was examined using a UV–vis spectrophotometer (model 2100 Series, Unico) at wavelength corresponding to the maximum absorbance of the MG (618 nm). Calibration curve was plotted based on the absorbance versus concentration of the standard MG solution using distilled water as a blank. Each experiment was done duplicate and the average values were recorded. The amount of MG adsorbed by nanozeolite CP was calculated according to following equation:

$$q_e = \frac{(C_0V_0 - C_eV_e)}{w} \quad (1)$$

where, $q_e$is the equilibrium concentration of MG adsorbed by nanozeolite which is known as MG uptake capacity (mg/g), C_0 and C_e are the initial and the equilibrium concentrations (mg/L) of MG, respectively; V_0 and V_e denotes initial and final volume of the solution (L), respectively and W is the weight of the adsorbent (g). Due to change in volume of solution during sampling, the initial and final volumes in Equation (1) have different values. The dye percent removal (%) was calculated using Equation (2):

$$\text{Removal}(\%) = \frac{C_0 - C_e}{C_0} \times 100 \quad (2)$$

3. RESULT AND DISCUSSION

3.1. Characterization of Raw Zeolite and Nanozeolite CP Table 1 summarized the chemical composition of raw zeolite which is determined by XRF. As it is observed, the main components included Si, O, Al, Ca, Fe, Na, Mg and small amount of S, Mn and P were also existed in adsorbent. In addition, 78 weight percentage of zeolite is components of SiO_2, Al_2O_3 and Fe_2O_3. Figure 1 depicts SEM images of nanozeolite CP. It can be observed that the obtained nanozeolite in some extent had circular shape and hetrogenous surface. The particle size was approximately between 36–40 nm. XRD pattern of nanozeolite is also depicted in Figure 2. The intensity ratio of the major peak observed at 2θ was 22°. The nanozeolite was demonstrated to be clinoptilolite by comparing with JCPDS data cards of clinoptilolite (01-083-1261). It demonstrated the crystalline structure of the nanozeolite powder. The main crystalline phase is related to SiO_2 and the phase of CaO, Fe_2O_3 and Al_2O_3 is also observed in samples structure. In addition, the XRD pattern depicts that the nanozeolite is clinoptilolite. FT-IR spectra of nanozeolite CP (Figure 3) revealed that the hydrogen bonds exist in the complex water-framework oxygen-cation around 3646.7 cm^{-1}. Broad band around 3434.6 cm^{-1} was because of stretching vibration of OH bond in hydroxyl groups. The peaks obtained at 1641.1 cm^{-1} was assigned to the bending H-O-H vibration. The peak located at 1087.7 cm^{-1} was characteristic of asymmetric stretching vibration of Si-O an Al-O bonds. The weak peak at 472.5 cm^{-1} was due to bending vibration of O-Si-O and O-Al-O.

3.2. Effect of Initial pH Solution One of the most key factors which control the adsorption process is pH solution values. Effect of initial pH (ranging 2 to 10) on adsorption of MG by nanozeolite was investigated. The experiments were conducted at a stirring speed of 150 rpm with initial MG concentration and adsorbent dosage of 20 mg/L and 0.2 g/L, respectively.

TABLE 1. The chemical component of raw zeolite obtained using XRF

Composition	SiO_2	Al_2O_3	Fe_2O_3	CaO	Na_2O	MgO	MnO	P_2O_5	SO_3	L.O.I
Weight percentage (%)	65.5	10.68	1.82	0.51	3.91	1.69	0.011	0.041	0.029	13.29

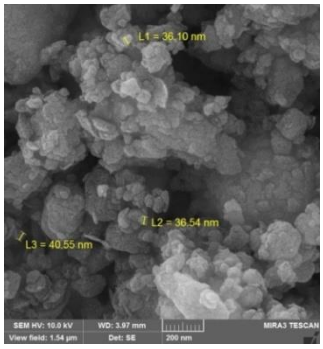

Figure 1. SEM image of the nanozeolite CP

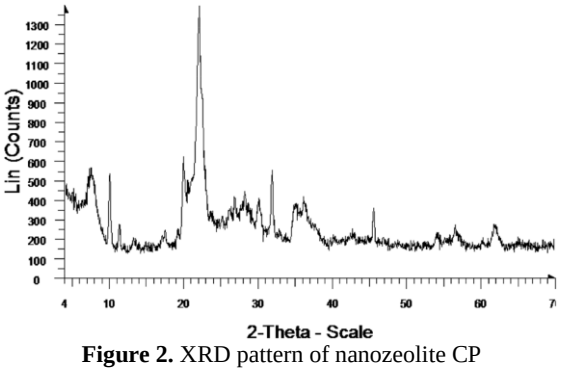

Figure 2. XRD pattern of nanozeolite CP

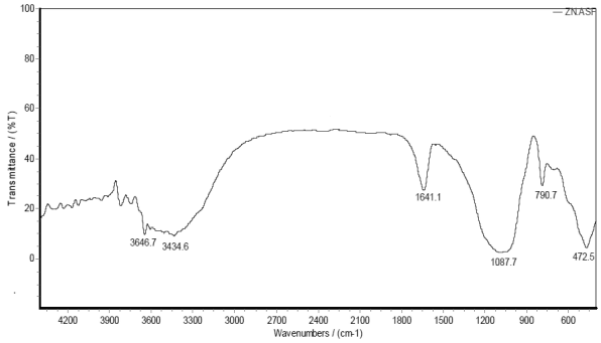

Figure 3. FT-IR spectra of nanozeolite CP

Figure 4 shows both removal efficiency and adsorption capacity increase with an increase in pH values. A Metrohm pH meter (model 827) with a combined double junction glass electrode was applied for showing pH values. The pH adjustments of the solution were done using the required amounts of 0.10 M HCl or NaOH solutions. The results revealed that a rise in pH from 2 to 8, the removal efficiency and adsorption capacity were increased from 72% and 7.76 mg/g to 96.2% and 9.7 mg/g, respectively. However, further increase in pH did not depict any appreciable improvement in removal efficiency and adsorbent capacity. The reason may be because of the presence of H^+ ions in acidic condition and ionization of the surface of adsorbent. As a result, the surface of adsorbent gains the positive charge and the tendency of adsorbent to MG adsorption decreases. Another reason may be due to competition between the H^+ ions and MG for the available active sites on nanozeolite surface in acidic condition and with loading the sites by H^+ ions, the MG removal decreases. In contrast, in alkali condition, the surface of adsorbent may be negatively charged which enhance adsorption of cationic dye to the adsorbent. Thus, the adsorbents had better operation in alkali condition. The maximum adsorption occurred at pH 8. Therefore, all the succeeding examinations were conducted at pH 8.

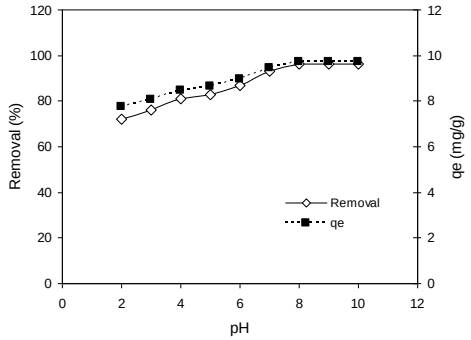

Figure 4. Effect of pH solution on MG adsorption (adsorbent dosage: 0.2 g; MG concentration: 20 mg/L; temperature: 30℃)

3. 3. Effect of Adsorbent Dose Adsorption process were performed at a fixed initial dye concentration of 20mg/L and various amounts of adsorbent ranging from 0.1 to 0.5 g/L with interval of 0.1. The pH solution was preadjusted to 8. Then, samples were shaken at 150 rpm and 30°C. Figure 5 shows the removal efficiency increased with an increase in adsorbent dose from 0.1 to 0.3 g/L, thereafter remained approximately constant in spite of an increase in amount of the adsorbent from 0.3 to 0.5 g/L. Actually, at high adsorbent dose, more adsorbent surface are available for MG dye to be adsorbed. Additionally, the adsorption capacity decreased with an increase in adsorbent dose from 0.1 to 0.5 g. It is owing to uncovering of more adsorbent active sites during the adsorption process, then the MG uptake capacity may decrease. It is in accordance with results reported in the literature [19]. At adsorbent dose of 0.3, removal efficiency reached to about 98%. Therefore, the adsorbent dose was fixed at 0.3g/L for all further experiments.

3. 4. Effect of Contact Time and Initial Dye Concentration Adsorption of MG into nanozeolite CP was done by regarding the effect of contact times for different initial MG concentrations from 10 to 50 mg/L. The removal percentages vs. contact time at various initial MG concentrations are presented in Figure 6.

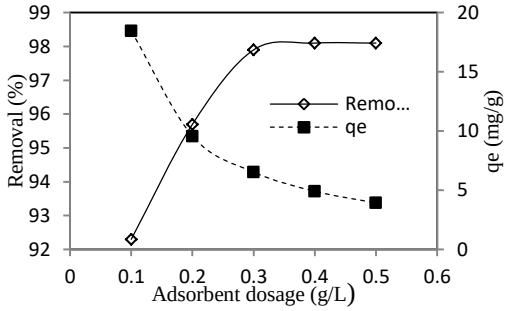

Figure5. Effect of absorbent dosage on MG removal (pH: 8; temperature: 30℃)

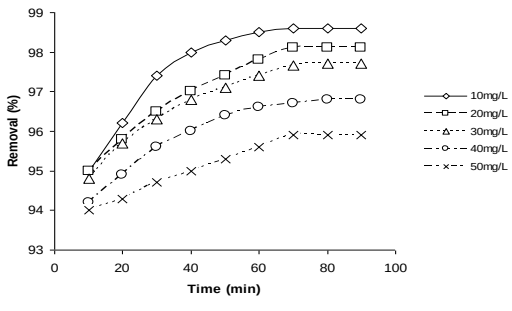

Figure 6. Effect of contact time on MG dye removal at various initial dye concentrations (absorbent dosage: 0.3 g; pH: 8; temperature: 30℃)

The plot shows that MG removal efficiency is higher at the beginning. This phenomenon is probably caused by a larger surface area of adsorbent exists at the beginning for MG adsorption. There is no significant variation on removal percentage, while the process reached to its equilibrium. At this time, the surface adsorption sites turn into exhausted, the uptake rate is controlled by the rate at which the MG is transported from the external to the internal sites of the nanozeolite. The achieved results showed that the maximum removal efficiency is 98.6% obtained at the equilibrium time of 70 min. In addition, the removal efficiency decreased from 98.6 to 95.9 % with an increase in MG concentration from 10 to 50 mg/L. At low MG concentration, the available sites for MG adsorption are high. MG was adsorbed on the empty sites of adsorbent surface and with an increase on MG concentration, the sites would be saturated. This is a frequent observed phenomenon referred commonly in adsorption literature [20].

3. 5. Adsorption Isotherms The adsorption isotherm is important to describe the interaction between an adsorbent and adsorbate. Five widely used isotherm models (Langmuir, Freundlich, Temkin, Dubinin-Radushkevich and Koble-Corrigan) were employed to explain the data achieved from the adsorption process. For isotherm analysis, experiments were accomplished by varying the initial MG concentration in the range of 10 to 50 mg/L.

3. 5. 1. Langmuir Isotherm Langmuir model assumes that uptake of MG molecules onto the adsorbent surface is homogeneous occurred by monolayer adsorption. Also, interaction between adsorbed molecules is negligible and a fixed number of adsorption sites are accessible. The linear form of the Langmuir isotherm is stated as follows [21]:

$$\frac{C_e}{q_e} = \frac{1}{q_m K_l} + \frac{C_e}{q_m} \quad (3)$$

where, q_m (mg/g) denotes to the monolayer adsorption capacity (mg/g) and K_l (L/mg) is Langmuir constant. The values of q_m and K_l determined by the slopes and intercepts of the plots of C_e/q_e vs. C_e (Figure 7a). The achieved parameters in different temperatures are summarized in Table 3. The essential characteristics of the Langmuir isotherm may be defined in terms of a dimensionless constant ($R_L = {}^{1}/_{1 + bC_0}$) referred to as equilibrium parameter or separation factor. b is the Langmuir constant (L/mg). The value of R_L depicts the nature of the isotherm which can be unfavourable (R_L>1), linear (R_L =1), favorable (0<R_L<1)or irreversible (R_L<0) [22].

Results showed that all the $R_L$values were between 0 and 1 indicating adsorption of MG onto nanozeolite CP is favorable at the conditions being studied. Maximum adsorption capacity of MG onto nanozeolite CP was 12.2 mg/g. Although, the value of MG adsorption capacity is not high comparing with other adsorbents [23]; but, nanozeolite CP is natural-based, cheap and easy available adsorbent to remove MG from aqueous solution.

3. 5. 2. Freundlich Isotherm Freundlich isotherm model is an empirical equation derived by assuming that there is a heterogeneous surface with a non-uniform distribution of energy of sorption over it. The linear form of Freundlich model can be expressed as stated in the following equation [24]:

$$logq_e = logK_f + \frac{1}{n} logC_e \quad (4)$$

where, K_f(mg/g(L/mg)$^{1/n}$) represents the Freundlich constant and n describes the heterogeneity of the adsorbent surface and its affinity for the adsorbate. Plot of logq_e vs. $logCe$is shown in Figure 7b. Values of n lies 1 to 10 indicated an effective and favorable bioadsorption process. Values of n close to or even 1 show the adsorbent with relatively homogenous binding sites. Although, high value of n depicts that there is a good adsorption over the all of concentrations studied, small n is donation of good adsorption at high concentrations but much fewer at lower concentrations. In addition, a higher value of K_f is a sign of a higher affinity of adsorbent for MG adsorption than a lower value. The values of K_f and n are presented in Table 3. Table 3 shows that nanozaolite CP was relatively a homogenous adsorbent. From the results, it was also clearly observed that the used adsorbent was well suited for MG adsorption and there is a good correlation between the experimental data and Freundlich model.

3. 5. 3. Temkin Isotherm Temkin isotherm (Equation (5)) attributed to the effects of various sorbate/adsorbate interactions on adsorption process. It proposed the linearly decrease of sorption heat for all molecules in the layer with coverage because of sorbate/sorbent interactions [25].

$$q_e = B\ln K_T + BlnC_e \qquad B = \frac{RT}{b} \quad (5)$$

where, $K_T$is the equilibrium binding constant (L/g) corresponding to the maximum binding energy, B is connected with heat of adsorption (J/mol), T is the absolute temperature (K) and R is the universal gas constant (8.314 J/mol K). The slope and intercept from a plot of q_e versus lnC_e determines the isotherm constants, K_T and B (Figure 7c).

3. 5. 4. Dubinin-Radushkevich (D-R) Isotherm The adsorption data were also applied to another adsorption isotherm, the Dubinin-Radushkevich (D-R) [26].

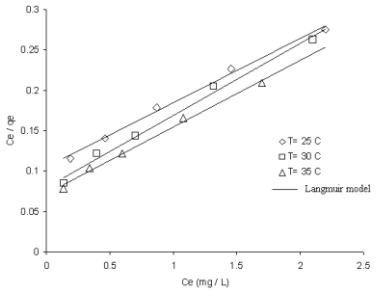

(a)

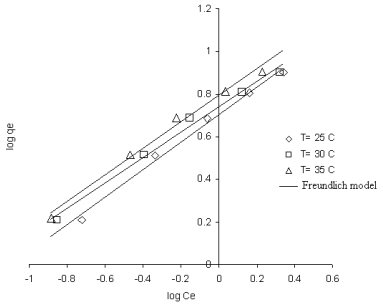

(b)

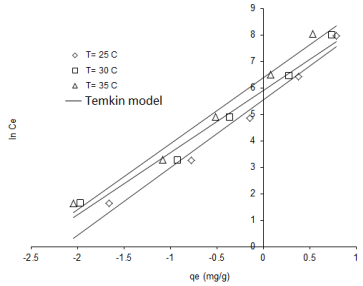

(c)

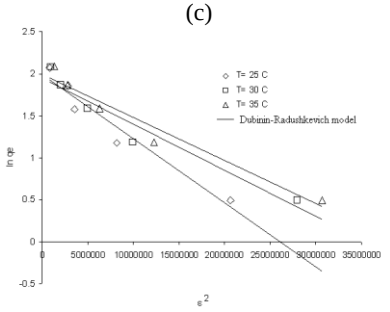

(d)

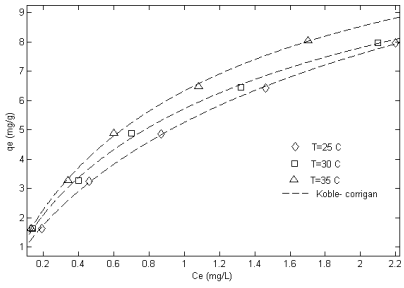

(e)

Figure 7. Sorption isotherms of MG onto nanozeoilite CP fitted to the (a) Langmuir (b) Freundlich (c) Temkin (d) Dubinin-Radushkevich and (e) Koble- Corrigan model at different temperatures (adsorbent dose = 0.3 g/L; pH: 8)

This isotherm is a more generalized model as compared to than the Langmuir isotherm. The D-R isotherm can be seen below as a linear form:

$$\ln(q_e) = \ln(q_{DR}) - B\varepsilon^2 \quad (6)$$

where, q_{DR} is the maximum adsorption capacity (mg/g) and B is the constant of adsorption energy (mol^2/kJ^2). The parameter ε is the polanyi potential which can be calculated by Equation (7). The model parameters were obtained by plotting lnq_e vs. ε^2 as shown in Figure 7d.

$$\varepsilon = RTln\left(1 + \frac{1}{C_e}\right) \quad (7)$$

3. 5. 5. Koble- Corrigan Isotherm The three-parameter Koble–Corrigan model which is a combination of the Langmuir and Freundlich models was used to express the adsorption data. It is represented by Equation (8) [27]:

$$q_e = \frac{AC_e^n}{1+BC_e^n} \quad (8)$$

TABLE 3. Isotherm models constants and correlation coefficients for the adsorption of MG onto nanozeolite CP

Isotherm models	T(℃)		
	25	**30**	**35**
Langmuir			
K_L (L/mg)	0.76	1.04	1.135
q_m(mg/g)	12.515	11.223	12.72
R^2	0.9946	0.9917	0.9948
Freundlich			
K_f(l/mg)	5.038	5.482	6.18
n	1.577	1.023	0.1.231
R^2	0.9914	0.9895	0.99
Temkin			
A(L/g)	8.597	12.074	12.663
B	2.5617	2.3461	2.4954
R^2	0.9805	0.9792	0.9818
Doubinin-Radushkevich			
q_{DR}(mg/g)	7.211	6.895	7.261
β(mol^2/kJ^2)	8×10^{-8}	5×10^{-8}	5.1×10^{-8}
R^2	0.9427	0.9390	9.163
Koble-Corrigan			
A	7.555	9.423	11.27
B	0.4374	0.6469	0.7796
n	0.8425	0.8351	0.8855
R^2	0.9996	0.9983	0.9991

where, *A*, *B* and *n* are the Koble–Corrigan parameters. As observed in Table 3, all R^2 values obtained for Koble–Corrigan model were bigger than 0.99, indicating well -fitting to the adsorption data. Considering studied isotherms, Langmuir, Freundlich, Temkin and Koble–Corrigan, it revealed that all of them were able to fit the experimental data. However, both Langmuir and Koble–Corrigan models were best used to fit the data.

3. 6. Adsorption Kinetics Most of the adsorption phenomena relay on time. The study of kinetic is required to optimize various operating conditions for adsorption of adsorbate on the adsorbent. In the current study, pseudo-first-order, pseudo-second-order and intraparticle diffusion models were tested to describe the adsorption kinetics behavior. The best fitted model was chosen based on the regression correlation coefficient (R^2). For kinetic adsorption experiment, 0.3 g/L of dry adsorbent was added to flasks containing 10, 20, 30, 40 and 50 mg/L MG as the initial concentration with pH adjusted to 8. Flasks were shaken at 150 rpm at three different temperatures (25, 30 and 35°C). Aliquot amounts of solution were taken from the shaker at appropriate time intervals. Residual MG concentrations in solutions were measured.

3. 6. 1. Pseudo-first Order Model The pseudo-first-order kinetic model is proposed to explain the adsorption kinetics. A linear form of pseudo-first order model is introduced as Equation (9):

$$\ln(q_e - q_t) = \ln(q_e) - k_1 t \quad (9)$$

where, k_1 denotes the equilibrium rate constant of pseudo-first order model (1/min). Figure 8a depicts plots of $\ln(q_e - q_t)$vs. t at 25℃. In addition, the values of rate constant k_1, q_e calculated, q_e experimental and R^2 at different temperature are shown in Table 4. There is none similarity between q_e calculated values and q_e experimental values which demonstrated that the sorption of MG is not expected to follow the pseudo-first-order kinetic model.

3. 6. 2. Pseudo-second Order Model The pseudo-second order equation developed as linear form as below [28]:

$$\frac{t}{q_t} = \frac{1}{k_2 q_e^2} + \frac{1}{q_e} t \quad (10)$$

where, k_2 shows the equilibrium rate constant of pseudo-second order kinetics (1/min). k_2 and q_e can be achieved from the intercept and slop of plotting $\frac{t}{q_t}$ vs. t. Figure 8b depicts plots of $\ln(q_e - q_t)$vs. t at 35℃. Table 4 also depicts the second order parameters k_2, q_e calculated and R^2 of MG adsorption onto nanozeolite. The q_e values calculated are very close to *qe* experimental. In addition, the obtained correlation values depicted that the pseudo-second-order kinetic model well fitted to kinetic data. The results revealed the pseudo-second-order kinetic model were able to fit kinetic data more than pseudo-first order model.

3. 6. 3. Intra-particle Diffusion Model The kinetic data were further tested to recognize the diffusion mechanism using the intraparticle diffusion model (Equation (11)) [29]. The rate controlling step of adsorption included three mass transfer steps: (1) external film diffusion, (2) intraparticle diffusion and (3) interaction step. Existence of multilinearity in the plot of uptake amount versus time square root would be an indicator of two or more steps in adsorption process. In fact, the overall rate of the process is controlled by the slowest step.

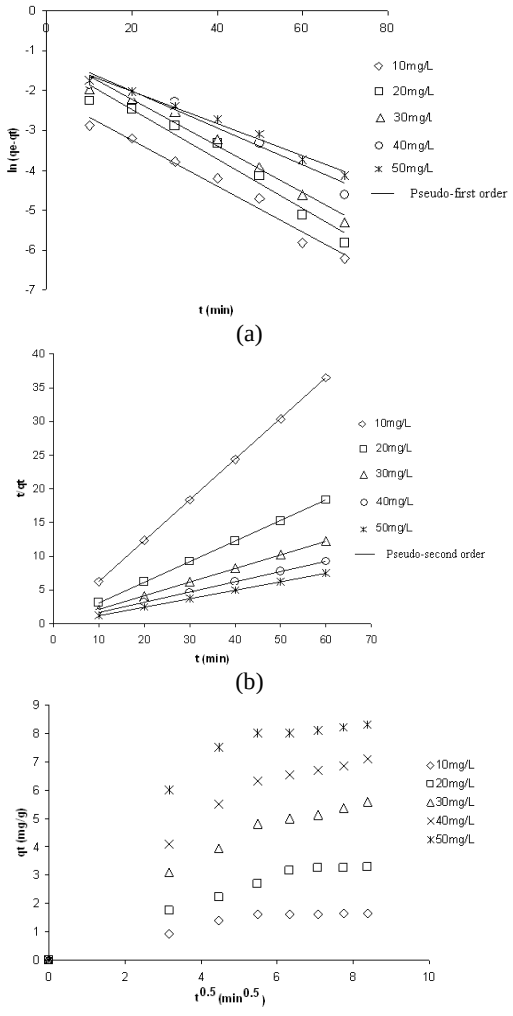

Figure 8. Pseudo-first-order, Pseudo-second-order and Intraparticle diffusion kinetic models of MG adsorption on nanozeolite CP at various concentrations and temperatures (a) 25℃, (b) 35 ℃ and (c) 30℃ , respectively

TABLE 4. Pseudo-first-order and pseudo-second-order kinetic model parameters for MG adsorption onto nanozeolite CP

T (℃)	C_0 (mg/L)	$q_{e(exp)}$(mg/g)	Pseudo- first order			Pseudo- second order		
			$q_{e(cal)}$(mg/g)	k_1(1/min)	R^2	$q_{e(cal)}$(mg/g)	k_2(g/mg min)	R^2
25	10	1.635	0.126	0.0578	0.9764	1.646	1.05	1
	20	3.256	0.291	0.0617	0.9577	3.279	0.49	1
	30	4.855	0.342	0.0578	0.9744	4.885	0.38	1
	40	6.423	0.334	0.0459	0.9583	6.447	0.376	1
	50	7.996	0.297	0.043	0.9847	7.994	0.315	1
30	10	1.643	0.195	0.0793	0.9477	1.657	1.105	0.9967
	20	3.267	0.205	0.0501	0.9385	3.316	0.510	0.9996
	30	4.883	0.253	0.0463	0.9809	4.91	0.406	1
	40	6.446	0.426	0.0645	0.9466	6.485	0.326	1
	50	7.983	0.287	0.0426	0.9283	8.0128	0.3408	1
35	10	1.645	0.1037	0.0802	0.9680	1.655	1.144	1
	20	3.276	0.177	0.0533	0.9557	3.297	0.635	1
	30	4.900	0.286	0.0536	0.9370	4.933	0.34	1
	40	6.487	0.359	0.0599	0.9467	6.5274	0.353	1
	50	8.050	0.347	0.0538	0.9063	8.091	0.325	1

$$q_t = k_{id} t^{0.5} + C \quad (11)$$

where, q_t is the amount of MG adsorbed onto nanozaolite at time t (mg/g), $t^{1/2}$ is the square root of the time, $K_{id}$is the intraparticle diffusion rate constant ($\mathrm{mg/g\,min^{1/2}}$) and C denotes the intercept and is correlated to the thickness of the boundary layer. Larger C represents the superior contribution of the boundary layer in the rate- controlling step. The slope of the plot of q_t versus $t^{1/2}$ verified the rate constant of intraparticle diffusion. If the plot passes through the origin, the rate limiting step will be only duo to the intraparticle diffusion. If not, some other mechanisms together with intraparticle diffusion are also contributed to the mechanism of the adsorption process. Figure 8c, the intraparticle diffusion plot, shows that the external surface sorption (step 1) is absent; because of the fast and instantaneous adsorption. It is possibly due to a strong interaction between MG and the external surface of adsorbent. In addition, all plotstrack the same common features, initial linear portion (step 2) followed by second linear one (step 3) and the linear lines of these stages did not pass through the origin. The second stage is intraparticle diffusion of MG through the pores of nanozeolite CP which is a gradual adsorption stage. The third stage is the final equilibrium stage which in intraparticle diffusion initiated to slow down maybe because of decreasing the MG concentration in the solution.

The achieved intraparticle rate constants and fitting correlation coefficients for the adsorption of MG on nanozeolite CP at 25, 30 and 35℃ for various MG initial concentrations are given in Table 5. It is shown that the k_{id} values for the two stages increase with an increase in temperature and dye initial concentration. It is resulted in because of enhancing the MG diffusion rate caused by an increase in the driving force. Furthermore, the results indicate that an increase in initial MG concentration from 10 to 50 mg/L and temperature at 25, 30 and 35℃ increase the intercept values. With regard to higher correlation coefficients, it can be concluded that the intraparticle diffusion mechanism as one of the rate controlling steps fitted well with the experimental data for the stage 2 of the adsorption process.

3. 7. Adsorption Thermodynamics Study on thermodynamics of an adsorption process provides precious knowledge which may be useful to describe an efficient operation. Temperature effect has been evaluated for the MG adsorption onto nanozeolite CP at various temperatures of 25, 30 and 35℃. The thermodynamic parameters, namely Gibbs free energy (Equation (12)), enthalpy change and entropy change have an important role to determine spontaneity and heat change for the adsorption process.

$$\Delta G^\circ = -RT \ln K_d \quad (12)$$

where, K_D depicts the distribution coefficient (mL/g) representing the progress of the adsorbate within the solution.

The values of K_d can be obtained from the following equation:

$$K_d = \frac{q_e}{C_e} \quad (13)$$

TABLE 5. Intraparticle diffusion kinetic model parameters for MG adsorption onto nanozeolite CP

T (℃)	C_0 (mg/L)	Intra particle diffusion					
		k_{id1}(mg/g min$^{1/2}$)	C_1(mg/g)	$(R_1)^2$	k_{id2}(mg/g min$^{1/2}$)	C_2 (mg/g)	$(R_2)^2$
25	10	0.2962	0.0196	0.9978	0.1157	0.9490	0.9497
	20	0.4699	0.0136	0.9972	0.0763	2.4354	0.9763
	30	0.7563	0.092	0.9964	0.1543	3.3789	0.9815
	40	0.9886	0.1125	0.9911	0.2421	5.3768	0.9761
	50	1.1267	0.1354	0.9981	0.2829	6.6741	0.9841
30	10	0.3012	0.0001	0.9973	0.005	1.6018	0.9506
	20	0.4931	0.0532	0.9957	0.0163	3.1318	0.9728
	30	0.8776	0.0874	0.9943	0.2895	3.1346	0.9775
	40	1.1721	0.1332	0.993	0.2687	4.8126	0.9722
	50	1.2562	0.1211	0.9979	0.3147	7.7698	0.9848
35	10	0.4542	0.0212	0.9981	0.1341	1.7201	0.9810
	20	0.5678	0.0721	0.9961	0.1563	4.5222	0.9761
	30	0.9121	0.1236	0.9871	0.3349	4.8321	0.9705
	40	1.2915	0.2781	0.9965	0.3971	6.2398	0.9721
	50	1.4904	0.3587	0.9704	0.4544	8.3437	0.9819

$$K_d = \frac{q_e}{C_e} \quad (13)$$

The enthalpy change ($\Delta H°$) and entropy change ($\Delta S°$) are calculated using the Van't Hoff's equation:

$$ln\, K_d = \frac{\Delta S°}{R} - \frac{\Delta H°}{RT} \quad (14)$$

The values of $\Delta H°$ and $\Delta S°$ were obtained from the slope and intercept of the Van't Hoff's plot of lnK_d versus $1/T$ as shown in Figure 9. The pseudo-second-order rate constant (k_2 (g/mg min)) as a function of temperature was used to evaluate the activation energy of adsorption by Arrhenius equation as below:

$$ln\, k_2 = lnk_0 - \frac{E_a}{RT} \quad (15)$$

where, E_a is the Arrhenius activation energy of adsorption (J/mol) and k_0 is a temperature independent (Arrhenius) factor (g/mg min). When lnk_2 is plotted vs. $1/T$, a straight line with the slope of $-E_a/R$ is achieved (see Figure 9). Thermodynamic parameters calculated for the adsorption of MG on nanozeolite CP are also summarized in Table 6.

$\Delta H°$ value is a helpful parameter to understand whether the process is an endothermic or exothermic. A positive $\Delta H°$ value indicates that the adsorption of MG onto nanozeolite CP is endothermic in nature which is in agreement with results obtained by Ahmad and Alrozi [20] that the MG uptakes increase with an increase in temperature. Furthermore, positive $\Delta S°$ value confirms the increased randomness at the liquid/solid interface during the adsorption of MG onto nanozeolite CP.

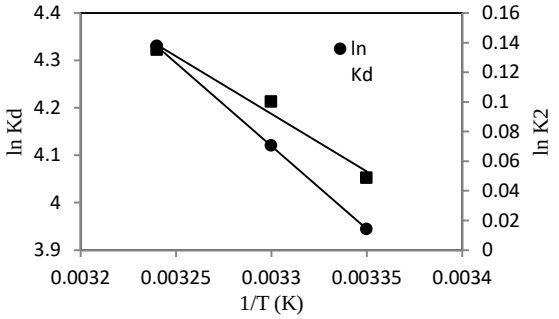

Figure 9. Plot of lnK_d and lnK_2 vs. $1/T$ for estimation of thermodynamic parameters and activation energy, respectively

TABLE 6. Thermodynamic parameters for MG adsorption onto nanozeolite CP

C_0 (mg/L)	$\Delta H°$ (kJ/mol)	$\Delta S°$ (kJ/mol)	E_a (kJ/mol)	$\Delta G°$ (kJ/mol))		
				298	303	308
10	28.5	0.129	6.46	-9.892	-10.54	-11.92

Concerning entropy concept, increasing in MG uptake capacity at higher temperatures can be regard to the enhance in mobility of MG ions. Thus, MG ions tend to transfer from the liquid phase to the solid phase at high temperature. The negative values of $\Delta G°$ revealed the feasibility of the process and also reflected that the process occurred spontaneously. A decrease in $\Delta G°$ from -9.892 kJ/mol to -11.92 kJ/mol with an increase in temperature from 25 to 35℃, respectively indicates more efficient adsorption at high temperature.

As mentioned in Table 6, E_a value was positive and was calculated to be 6.46 kJ/mol. When E_a value is 8–

16 kJ/mol, the adsorption process is tracked by chemical process, but when E_a< 8 kJ/mol, the adsorption process is physical in nature. On the other hand, when E_a> 16 kJ/mol, particle diffusion is significant. Therefore, physical process may be control the rate-limiting step in the MG adsorption onto nanozeolite CP. In fact, physical adsorption reaches to the thermodynamic equilibrium rapidly compared with chemical adsorption.

4. CONCLUSION

The present study shows the effectiveness of cheap and nano-sized natural zeolite CP to adsorb MG from aqueous solution. Nanozeolite was obtained using a fast, simple and low cost method. In Table 7, the adsorption capacity of nano-sized natural zeolite CP was compared with some adsorbents reported for the removal of MG in literatures [9, 30-34]. The results revealed that adsorption of MG by nanozeolite CP were strongly depends on initial pH solution. The pH value of 8 was found to be an optimum for the adsorption process. The adsorption of MG was observed to increase with a rise in contact time, initial MG concentration and solution temperature. Based on values of fitting correlation coefficients, Koble-Corrigan isotherm and the pseudo-second-order kinetic models resulted in a better fit to the adsorption data. The intraparticle diffusion model demonstrated to be as one of the rate-controlling steps during adsorption. In addition, thermodynamic studies indicated the spontaneous and endothermic nature of adsorption process.

TABLE 7. Comparison of adsorption capacity of nanozeolite CP with some adsorbents for the removal of MG

Adsorbent	Maximum adsorption capacity (mg/g)	Adsorbent dose (g/L)	Contact time (min)	pH	Temperature (K)	Reference
Natural zeolite	26.36	-	-	-	-	[30]
Natural zeolite	5×10^{-5} (mol/g)	-	-	6	303	[31]
Alg–Fe3O4 nanoparticles	47.84	0.1 (in 50 ml)	-	9	-	[32]
Polyaniline–nickel ferritemagnetic nanocomposite	4.09	5	210	7	-	[33]
Modified nano-γ-alumina	72.4	0.8	-	3	298	[34]
Nanozeoliteclinoptilolite	12.72	0.3	70	8	308	This work

5. ACKNOWLEGMENT

The authors gratefully acknowledge the facilities provided to carry out research at Islamic Azad University, Ayatollah Amoli Branch.

6. REFERENCES

1. Dezhampanah, H., Mohammad-khah, A. and Aghajani, N., "Equilibrium and thermodynamic studies of thionine adsorption from aqueous solution onto rice husk", ***European Chemical Bulletin***, Vol. 2, (2014), 709-714.
2. Ajemba, R. O., "Adsorption of Malachite Green from Aqueous Solution using Activated Ntezi Clay: Optimization, Isotherm and Kinetic Studies", ***International Journal of Engineering***, Vol. 27, No. 6, (2014), 839-854.
3. Bharathi, K. and Ramesh, S., "Removal of dyes using agricultural waste as low-cost adsorbents: a review", ***Applied Water Science***, Vol. 3, (2013), 773-790.
4. Baldez, E.E., Robaina, N.F. and Cassella, R.J., "Employment of polyurethane foam for the adsorption of Methylene Blue in aqueous medium", ***Journal of Hazardous Material***, Vol. 159, (2008), 580-586.
5. Mishra, G. and Tripathy, M., "A critical review of the treatment for decolorization of dye wastewater", ***Colourage***, Vol. 40, (1993), 35-38.
6. Wang, X.S., Zhou, Y., Jiang, Y. and Sun, C., "The removal of basic dyes from aqueous solutions using agricultural by-products", ***Journal of Hazardous Material***, Vol. 157, (2008), 374-385.
7. Dezhampanah, H., Mousazadeh, A. and Mousazadeh, I., "Sugarcane Bagasse and Modified Rice Husk for the Removal of Malachite Green from Aqueous Wastes", ***European Chemical Bulletin***, Vol. 3, (2013), 400-406.
8. Ngah, W., Saime, W., Ariff, N.F.M., Hashim, A. and Hanafiah, M.A.K.M., "Malachite green adsorption onto chitosan coated bentonite beads: isotherms, kinetics and mechanism", ***Clean-Soil, Air, Water***, Vol. 38, (2010), 394-400.
9. Agarwala, S., Nekoueib, F. Kargarzadehc, H., Nekoueib, S., Tyagid, I. and Gupta, V.K., "Preparation of Nickel hydroxide nanoplatesmodified activated carbon for Malachite Greenremoval from solutions: Kinetic, thermodynamic,isotherm and antibacterial studies", ***Process Safety and Environmental Protection***, Vol. 102, (2016), 85-97.
10. Humelnicu, I., Baiceanu, A., Ignat, M.E. and Dulman, V., "The Removal of Basic Blue 41 Textile Dye from Aqueous Solution by Adsorption onto Natural Zeolitic Tuff: Kinetics and Thermodynamics", ***Process Safety and Environmental Protection,*** Vol. 105, (2017), 274–287.
11. Han, R., Ding, D., Xu, Y., Zou, W., Wang, Y., Li, Y. and Zou, L., "Use of rice husk for the adsorption of congo red from aqueous solution in column mode", ***Bioresource Technology***, Vol. 99, (2008), 2938-2946.
12. Mall, I.D., Srivastava, V.C., Agarwal, N.K. and Mishra, I.M., "Adsorptive removal of malachite green dye from aqueous solution by bagasse fly ash and activated carbon-kinetic study and equilibrium isotherm analyses", ***Colloids and Surfaces A: Physicochemical and Engineering Aspects,*** Vol. 264, (2005), 17-28.
13. El Qada, E.N., Allen, S.J. and Walker, G.M., "Adsorption of basic dyes from aqueous solution onto activated carbons", ***Chemical Engineering Journal***, Vol. 135, (2008), 174-184.

14. Walker, G. and Weatherley, L., "Textile wastewater treatment using granular activated carbon adsorption in fixed beds", ***Separation Science and Technology,*** Vol. 35, (2000), 1329-1341.
15. Samiey, B. and Toosi, A.R., "Adsorption of malachite green on silica gel: Effects of NaCl, pH and 2-propanol", ***Journal of Hazardous Materials,*** Vol. 184, (2010), 739-745.
16. Zanin, E., Scapinello, J., de Oliveira, M., Rambo, C.L., Franscescon, F., Freitas, L., de Mello, J.M.M., Fiori, M.A., de Oliveira, J.V. and Dal Magro, J. "Adsorption of heavy metals from wastewater graphicindustry using clinoptilolite zeolite as adsorbent", ***Process Safety and Environmental Protection,*** Vol. 105, (2017), 194–200.
17. Kallo, D., Papp, J. and Valyon, J., "Adsorption and catalytic properties of sedimentary clinoptilolite and mordenite from the Tokaj Hills, Hungary", ***Zeolites***, Vol. 2, (1982), 13-16.
18. Baghbanian, S.M., Rezaei, N. and Tashakkorian, H.,. "Nanozeolite clinoptilolite as a highly efficient heterogeneous catalyst for the synthesis of various 2-amino-4 H-chromene derivatives in aqueous media", ***Green Chemistry,*** Vol. 15, (2013), 3446-3458.
19. Jeon, C. and Park, K.H., "Adsorption and desorption characteristics of mercury (II) ions using aminated chitosan bead", ***Water Research***, Vol. 39, (2005), 3938-3944.
20. Ahmad, M.A. and Alrozi, R., "Removal of malachite green dye from aqueous solution using rambutan peel-based activated carbon: Equilibrium, kinetic and thermodynamic studies", ***Chemical Engineering Journal,*** Vol. 171, (2011), 510-516.
21. Langmuir, I., "Constitution and fundamental properties of solids and liquids. I: solids", ***Journal of Hazardous Materials,*** Vol. 139, (2007), 57-66.
22. Weber, T.W. and Chakravorti, R.K., "Pore and solid diffusion models for fixed-bed adsorbers", ***AIChE Journal,*** Vol. 20, (1974), 228-238.
23. Das, D. and Pal, A., "Adsolubilization phenomenon perceived in chitosan beads leading to a fast and enhanced malachite green removal", ***Chemical Engineering Journal***, Vol. 290, (2016), 371-380.
24. Freundlich, H., "Over the adsorption in solution", ***The Journal of Physical Chemistry A***, Vol. 57, (1906), 1100-1107.
25. Temkin, M. and Pyzhev, V., "Recent modifications to Langmuir isotherms",***ActaPhysiochimica U. S. S. R.,*** Vol. 12, (1940), 217-222.
26. Polyzopoulos, N., Keramidas, V. and KiossE, H., "Phosphate sorption by some alfisols of Greece as described by commonly used isotherms", ***Soil Science Society of America Journal***, Vol. 49, (1985), 81-84.
27. Koble, R.A. and Corrigan, T.E., "Adsorption isotherms for pure hydrocarbons", Ind. Eng. Chem. Vol. 44, (1952), 383-387.
28. Ho, Y.S. and McKay, G., "Pseudo-second order model for sorption processes", ***Process Biochemistry***, Vol. 34, (1999), 451-465.
29. Weber, W.J. and Morris, J.C., "Kinetics of adsorption on carbon from solution***", Journal of Sanitary Engineering Division,*** Vol. 89, (1963), 31-60.
30. Wu, X., Wang, Y., Liu, J., Ma, J. and Han, R., "Study of malachite green adsorption onto natural zeolite in a fixed-bed column", ***Desalination and Water Treatment***, Vol.20, (2010), 228–233.
31. Wang, S., Ariyanto, E., "Competitive adsorption of malachite green and Pb ions on natural zeolite", ***Journal of Colloid and Interface Science***, Vol. 314, (2007), 25–31.
32. Mohammadi, A., Daemi, H., Barikani,M., "Fast removal of malachite green dye using novel superparamagnetic sodium alginate-coated Fe_3O_4 nanoparticles", ***International Journal of Biological Macromolecules***, Vol. 69, (2014), 447-55.
33. Patil, M.R. and Shrivastava, V.S., "Adsorption of malachite green by polyaniline–nickel ferrite magnetic nanocomposite: an isotherm and kinetic study", ***Applied Nanoscience***, Vol. 5, (2015), 809–816.
34. Mohammadifar, E., Shemirani, F., Majidi, B., Ezoddin, M., "Application of modified nano-γ-alumina as an efficient adsorbent for removing malachite green (MG) from aqueous solution", ***Desalination and Water Treatment***, Vol. 54, (2014), 758-768.

Adsorption of Malachite Green from Aqueous Solution by Nanozeolite Clinoptilolite: Equilibrium, Kinetic and Thermodynamic Studies

R. Heydari[a], M. Khavarpour[b]

[a]Department of Chemical Engineering, South Tehran Branch, Islamic Azad University, Tehran, Iran
[b]Department of Chemical Engineering, Ayatollah Amoli Branch, Islamic Azad University, Amol, Iran

P A P E R I N F O

Paper history:
Received 29September 2017
Received in revised form 23October 2017
Accepted 30November 2017

Keywords:
Adsorption Kinetics
Thermodynamics
Malachite Green
Nanozeolite Clinoptilolite
Isotherm Models

چکیده

هدف از مطالعه حاضر، بررسی پتانسیل جذب نانو زئولیت کلینوپتیلولیت (CP) برای حذف مالاچیت گرین (MG) از فاز آبی در یک سیستم تعادلی ناپیوسته است. تکنیکهای SEM، EDX، XRF، XRD و FT-IR برای مشخص کردن خصوصیات زئولیت استفاده شد. اثرات pH اولیه محلول، دوز جاذب، دما، زمان تماس و غلظت اولیه MG در جذب مورد بررسی قرار گرفت. آزمایش های جذب در محدوده غلظت های اولیه ۱۰-۵۰ میلی گرم در لیتر در دمای ۲۵، ۳۰ و ۳۵ درجه سانتیگراد انجام شد. میزان جذب MG با افزایش زمان تماس، غلظت اولیه MG و دمای محلول افزایش یافت. داده های تعادلی جذب مناسب ترین تطابق را با مدل کوبل-کوریگان نشان دادند. سینتیک MG روی جاذب از مدل شبه درجه دوم پیروی کرد. علاوه بر این، ارزیابی داده های سینتیکی نشان داد که میزان جذب توسط مکانیسم نفوذ درون ذره ای کنترل می شود. مقادیر منفی انرژی آزاد گیبس استاندارد، جذب خود به خودی را در دماهای مورد مطالعه نشان داد. مقادیر مثبت تغییرات آنتالپی و آنتروپی نیز تصادفی بودن و طبیعت گرماگیر بودن جذب MG را بر روی جاذب نانوزئولیت CP تأیید می کنند. علاوه بر این، انرژی فعال به دست آمده، روند جذب فیزیکی را نشان می دهد.

***doi**: 10.5829/ije.2018.31.01a.01*